

# Modification of the CHARMM Force Field for DMPC Lipid Bilayer

CARL-JOHAN HÖGBERG,<sup>1</sup> ALEXEI M. NIKITIN,<sup>1,2</sup> ALEXANDER P. LYUBARTSEV<sup>1</sup>

<sup>1</sup>*Division of Physical Chemistry, Arrhenius Laboratory, Stockholm University, Stockholm, SE-10691, Sweden*

<sup>2</sup>*Engelhardt Institute of Molecular Biology, Russian Academy of Sciences, Moscow 119991, Russia*

Received 23 August 2007; Revised 8 February 2008; Accepted 10 February 2008

DOI 10.1002/jcc.20974

Published online 29 May 2008 in Wiley InterScience (www.interscience.wiley.com).

**Abstract:** The CHARMM force field for DMPC lipids was modified in order to improve agreement with experiment for a number of important properties of hydrated lipid bilayer. The modification consists in introduction of a scaling factor 0.83 for 1–4 electrostatic interactions (between atoms separated by three covalent bonds), which provides correct transgauche ratio in the alkane tails, and recalculation of the headgroup charges on the basis of HF/6-311(d,p) *ab-initio* computations. Both rigid TIP3P and flexible SPC water models were used with the new lipid model, showing similar results. The new model in a 75 ns simulation has shown a correct value of the area per lipid at zero surface tension, as well as good agreement with the experiment for the electron density, structure factor, and order parameters, including those in the headgroup part of lipids.

© 2008 Wiley Periodicals, Inc. J Comput Chem 29: 2359–2369, 2008

**Key words:** molecular dynamics; lipid bilayers; force field; DMPC; hydration

## Introduction

Molecular computer simulations of lipid membrane bilayers have attracted much attention during the last decade, because of the role of lipid membranes play in living organisms.<sup>1–7</sup> Clearly, outcome of simulations is very much dependent on the quality of the force field which is used to simulate the system. Most of simulations carried out up to date used different variations of the GROMOS force field with the united atom model.<sup>2,3</sup> While giving generally fair representation of the bilayer structure and dynamics, the GROMOS force field still has some disagreement with the experimentally observable properties. Small, but going beyond possible computational or experimental error differences have been noted for the electron density profile (or the structure factor), area per lipid, order parameters, and some other properties.<sup>8,9</sup> Some of these disagreements could be probably removed by further optimization of the force field parameters. It may be also argued that the observed differences are related to the use of a united atom representation of methyl or methylene groups in the GROMOS force field. There exists experimental data showing possible formation of hydrogen bonds between hydrogens of choline group and water.<sup>10</sup> It is also known that there may exist a weak attractive minima in between hydrogen atoms of methyl or methylene groups. Explicit hydrogens attached by flexible bonds to carbon atoms may be also important for accurate description of the *CH* or *CD* order parameters. A good quality all atomic model seems

to be necessary in order to address such details in the description of lipid bilayers.

Another frequently used force field for simulations of lipid bilayers is the CHARMM force field.<sup>11</sup> In addition to explicit presence of all hydrogens, the CHARMM force field has a more detailed description of intramolecular interactions, including Urey-Bradley term for covalent angles, and a richer variety of parameters for dihedral angles, many of which being developed on the basis of quantum-chemical calculations. From this point of view the CHARMM force field can have advantages in accurate description of lipid bilayers. However, recent detailed investigations have shown that the CHARMM force field have also disagreements with the experiment.<sup>8</sup> It was found for example, that such fundamental parameter as the average area per lipid, is underestimated in constant-pressure simulations with the CHARMM force field.<sup>12,13</sup> Recently an update of CHARMM27 torsion parameters for alkane chains (the so-called *c27r* parameter set) has been suggested,<sup>14</sup> but according to a subsequent paper,<sup>15</sup> the *c27r* parameter set still does not reproduce the correct area per lipid in simulations at zero surface tension. Also, an attempt was made to recalculate charges of the lipid headgroup.<sup>16</sup>

**Correspondence to:** A. P. Lyubartsev; e-mail: alexander.lyubartsev@physc.su.se

Contract/grant sponsor: Swedish Research Council (Vetenskapsrådet)

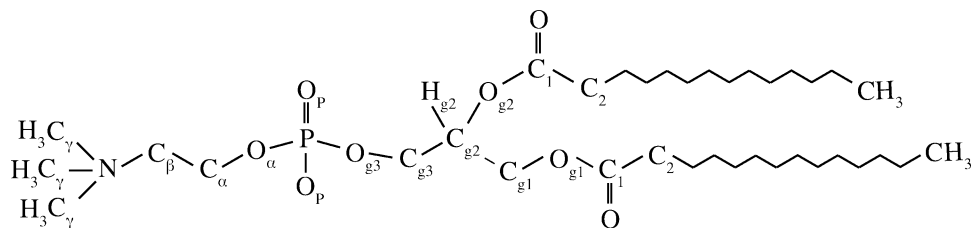


**Figure 1.** The DMPC molecule with atom labels used in the text.

Though recalculation of charges has brought results closer to the experiment, the resulting area per lipid was still about  $4\text{--}5 \text{ \AA}^2$  too low, both for DPPC<sup>13</sup> and DMPC<sup>17</sup> lipids. Our test simulations have also showed too ordered, gel-like structures with too low area per lipid while simulating DMPC bilayer under condition of zero surface tension.

We have decided to investigate some modifications of the CHARMM force field in order to bring simulation results for lipid bilayers closer to the experiment. The first attempt of the modification was a change of the water model. The CHARMM force field uses by default the TIP3P<sup>18</sup> model for water. This model is rigid, which is not quite consistent with the description of other molecules as flexible. Moreover, the TIP3P model has a too high dielectric permittivity evaluated as  $\epsilon = 97 \pm 6$ .<sup>19</sup> The last feature means in fact that the electrostatic interactions may be effectively underestimated if this water model is used. The average area per lipid, observed in constant pressure simulations, is rather sensitive to the way on how the long-range electrostatic interactions are treated.<sup>5,20</sup> From this point of view, it may be important to use a water model having dielectric permittivity close to the experimental. Recently some modifications of the TIP3P model have been suggested<sup>21</sup> which provide their lower dielectric permittivity, closer to the experimental one. We however have chosen the flexible SPC water model.<sup>22</sup> In addition to a correct dielectric permittivity (evaluated as  $\epsilon = 82 \pm 4$  in<sup>23</sup> and  $\epsilon = 78 \pm 2$  at 298 K according to<sup>24</sup>), this model, due to its flexibility, can change the dipole moment in the response to a change of environment, and thus mimic polarizability. The latter feature makes the flexible SPC model more advantageous for simulation of water both in the bulk environment and in contact with polar or hydrophobic parts of lipids.

A simple substitution of the TIP3P model by the flexible SPC model in simulation of a fully hydrated DMPC bilayer has led however to worsening of the results: the average area per lipid was reduced even more (a detailed description of the simulations made and the obtained results is given later). It became clear that further improvements of the model were necessary. We found from the analysis of the results for nonmodified CHARMM27 lipid model that the fraction of gauche defects in lipid tails was too low, with values typical for a gel phase. The probable reason for this could be a too low energy of the trans-conformation of the hydrocarbon chain in comparison with the energy of the gauche-conformation. In fact, recent modification of the CHARMM27 force field<sup>14</sup> aimed just to increase the fraction of gauche-conformations, but it seems that this increase was not enough. We investigated in more details how the flexibility of the lipid tails, defined by the relative energies of trans and gauche conformations, affects the average area per lipid and other properties of the lipid bilayer. The relative energies

of trans and gauche conformations can be conveniently varied by a scaling parameter for the so-called 1–4 electrostatic interactions (that is electrostatic interactions between atoms separated by three covalent bonds). A decrease of this parameter leads to an increase of the gauche-trans fraction and to a general increase of the chain flexibility. Additional simulations with varying 1–4 electrostatic scaling parameter were carried out for liquid hexadecane.

The simulations showed that indeed, a decrease of 1–4 electrostatic scaling parameter leads to a higher fraction of gauche conformations and to a larger area per lipid. It turned out however that the value of the 1–4 scaling factor, which provides the best agreement with the experimentally known fraction of gauche conformations in the lipid tails and in liquid hexadecane, still yields a too low average area per lipid. Therefore, a next step in optimization of the force field was made. We recalculated partial atom charges for the whole lipid headgroup including esters using Hartree-Fock (HF/6-311(d,p) level) quantum-chemical theory. These computations were made for a number of lipid configurations randomly chosen from previous bilayer simulations. Similar approach was very recently applied for reparametrization of charges in DPPC lipid,<sup>13</sup> with computations made on the RHF/6-31G(d) level. The new partial charges were used in the final model, together with the scaling factor for 1–4 electrostatic interactions which provided the best trans-gauche ratio in alkane chain simulations. The formulated, in this way, model yielded not only the correct average fraction of gauche conformations in the lipid tails, but provided also a good agreement with experiment for the area per lipid, electron density, X-ray structure factor, and the NMR order parameters.

The paper is organized as follows. In Section “Computational Details”, the details of the computational procedures are given. In Section “Effect of Scaling of 1–4 Electrostatic Interactions on Bilayer Structure”, the effect of 1–4 electrostatic scaling parameters on lipid tails flexibility and on other properties of bilayer is discussed. In Section “Hexadecane simulations”, the value of 1–4 electrostatic scaling factors providing the best agreement with experiment for hexadecane is derived. Section “Optimization of atom charges” contains details on quantum-chemical reparametrization of charges for the lipid headgroup. Results of simulations of the finally modified lipid model and their comparison with experiment are described in Section “Simulation of DMPC Bilayer with Reparametrized charges”. The overall discussion of the obtained results and conclusions are given in last section.

## Computational Details

All lipid bilayer simulations have been carried out for 98 DMPC (dimyristoylphosphatidylcholine) lipids shown in Figure 1 and

organized in a bilayer (49 lipids in each leaflet), hydrated by 2700 water molecules.

The CHARMM27 force field (as specified in supporting information of<sup>25</sup>) was used for description of lipids, including all its special features as Urey-Bradley term for intramolecular vibrations, improper dihedral angles, and special Lennard-Jones parameters for atoms separated by three covalent bonds. For water, anharmonic flexible SPC model was used.<sup>22</sup> The finally formulated lipid model was simulated also in the presence of rigid TIP3P water.<sup>18</sup> The Lorentz-Berthelot combination rule<sup>26</sup> was used to describe Lennard-Jones interactions between unlike atoms. Note, that the Lennard-Jones parameters of the TIP3P and SPC water are almost identical, that is why the change of the water model practically does not affect the Lennard-Jones interactions, but affect the electrostatics. The modification of the CHARMM force field, described in details later, included introduction of a scaling factor for electrostatic interactions between 1–4 neighbours (in CHARMM, these interactions are not scaled), and, in “Simulations of DMPC Bilayer with Reparametrized Charges”, a change of partial atom charges.

The system was simulated in a rectangular periodic box. The Nose-Hoover constant pressure–constant temperature time reversible algorithm, with separate box size fluctuations along each direction, was applied.<sup>27</sup> In all simulations, the temperature was set to 303 K and the pressure to 1 atm.

The double time step algorithm<sup>28</sup> was used to treat separately fast (covalent bonds, angles, torsions and collision Lennard-Jones forces within 5 Å distance) and slow forces, with the 0.25 fs time step for the fast and 2 fs time step for the slow forces. In fact, integration of the fast forces takes only a small fraction of the total cpu time, and such an algorithm, allowing to treat completely flexible models, takes in fact almost the same cpu time as dynamics with constrain covalent bonds and 2 fs time step.

The electrostatic interactions were treated by the Ewald summation method.<sup>26,29</sup> The cut-off distance for the real-space part of the Ewald sum, as well as for the Lennard-Jones interactions, was set to 13 Å. The reciprocal part of the Ewald sum was cut at the condition that the remaining terms do not contribute more than on 0.0001 level of the total value. The dispersion correction from the Lennard-Jones interactions outside the cut-off was included into the pressure.

In the beginning, the lipids were organized into bilayer in an ordered manner, and the water molecules were added from the both side. Then, a nanosecond simulation was made in which the box sizes were gradually brought to the experimentally expected values (corresponding to the area per lipid of 60 Å<sup>2</sup> and 62 Å in the normal direction). Then, a 1 ns simulation with isotropic cell fluctuations has been performed. The obtained in this way configuration was used as a start point for subsequent simulations.

Additional simulations of liquid hexadecane have been carried out for 216 hexadecane molecules described by the same CHARMM27 force field for lipids. The simulations were performed in a cubic box with isotropic cell fluctuations. Equilibration time was 500 ps and average collection 1 ns. All other molecular dynamics features were the same as in the described above bilayer simulations.

Most of simulations have been carried out by the MDynaMix package v.4.4.<sup>30</sup> For some simulations mentioned separately, GROMACS v.3.2<sup>31</sup> and NAMD v.2.6 packages<sup>32</sup> were used.

## Effect of Scaling of 1–4 Electrostatic Interactions on Bilayer Structure

When the bilayer was simulated with unmodified CHARMM force field (but with the flexible SPC water), the average area per lipid was contracted to about 48 Å<sup>2</sup> in a few nanoseconds, see the lowest line in Figure 2. This is clearly below the experimental value for the liquid crystalline phase and corresponds in fact to the value of the area in a gel phase. Even visual inspection of the configurations showed highly ordered conformations with lipid tails well aligned relative to each other.

There exist many different ways to vary force field parameters in order to get desirable changes in the structure. We began from the part which showed the most noticeable deviations from the expected behavior: the lipid tails which were too much ordered, with only a small (14%) fraction of gauche-conformations of the hydrocarbon chain. According to FTIR spectroscopic measurements carried out for DLPC and DPPC lipids in the liquid crystalline phase just above the phase transition point, the total fraction of gauche defects is in the range of 25–30%,<sup>33,34</sup> while the 14% ratio is more relevant for the gel phase. That is why modification of the force field leading to a higher fraction of gauche conformations seems to be necessary. Note, that recent modification of CHARMM parameters<sup>14</sup> was made just with such a purpose: the *c27r* parameter set defined in that work had somewhat smaller difference in energy between trans and gauche conformations. We decided to vary the ratio between trans and gauche conformations by varying the scaling factor for 1–4 electrostatic interactions. Though the partial atomic charges on the atoms of hydrocarbon chains are small (0.09 on hydrogens and –0.18 on carbons), they make a noticeable contribution into the total energy change upon rotation of the torsional angle. It is not difficult to realize, that an overall effect of electrostatic interactions between the atoms separated by three covalent bonds favors to transconformations. Since the original CHARMM force field uses nonscaled 1–4 electrostatic interactions, scaling down these interactions would change the balance in favor of gauche conformations.

Clearly, there is no fundamental reason for why 1–4 electrostatic interactions should be scaled down. There are many other ways to change the balance between trans and gauche conformations, such as changes of 1–4 Lennard-Jones interactions, change of the explicit dihedral potential, etc. The approach we adopted is just one simple way to adjust the effective dihedral potential using a single parameter.

The effect of scaling of 1–4 electrostatic interaction on the total torsion potential energy of a hydrocarbon chain is illustrated in Figure 3. We displayed in this figure the potential energy of an isolated hexane molecule, with all the bonds, angles and torsions in the equilibrium positions, except the torsion angle in the middle of the molecule (2-3-4-5 carbons), which is changing between 0° and 180°. In all cases, transconformation of this torsion angle is accepted as zero of energy. One can see that when the scaling factor is changing from 1 to 0.6, the difference in energy between gauche and trans conformations is decreasing from 4.4 kJ/mol to 1.7 kJ/mol, making gauche conformation more favorable. For comparison, we display also the potential energies computed within the *c27r* force field,<sup>14</sup> and those using the Ryckaert-Bellemans torsion potential with Lennard-Jones parameters of the united atom GROMOS force field as described in article.<sup>3</sup>

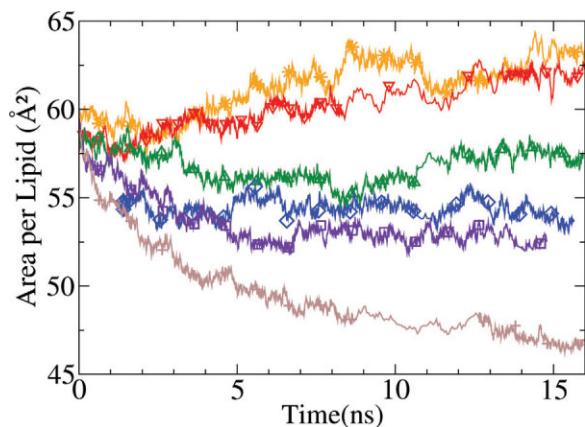


**Figure 2.** Area per lipid for systems simulated with different values of 1–4 electrostatic scaling factors: 0.5, orange with stars; 0.6, red with triangles down; 0.7, green with triangles up; 0.8, blue with diamonds; 0.9, violet with squares; 1, brown with pluses.

We have carried out six simulations in which the scaling factor  $\alpha_{14}$  for 1–4 electrostatic interactions was changed from 1 to 0.5 with step 0.1. The evolution of the average area per lipid in each case is shown in Figure 2. It is evident that the 1–4 scaling factor affects the area per lipid dramatically: a decrease of this factor leads to a strong increase of the area, which for scaling factors 0.6 and 0.5 becomes above the experimental value.

One can see that after 5–10 ns of simulation the area per lipid approaches to a stable level. The total simulation length may still not be enough to say about true equilibration, but the observed trends clearly show, that the experimental value of the area per lipid corresponds to a value of scaling factor  $\alpha_{14}$  between 0.6 and 0.7. To understand whether such a value is realistic, we computed a number of other observable properties over the last 5 ns in each of the cases,

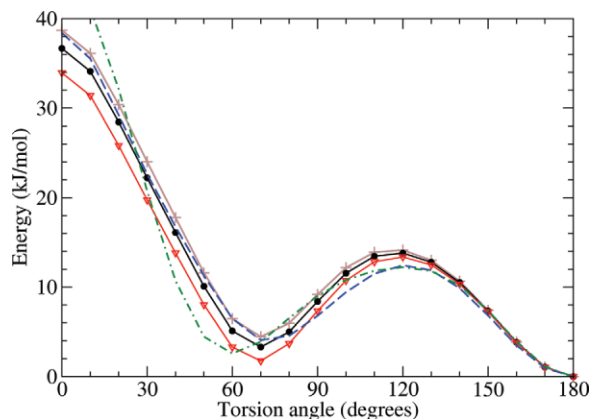


**Figure 3.** Potential energy of hexane molecule upon rotation of the central torsion angle with equilibrium values of bond lengths, covalent and other torsion angles. The zero of energy corresponds to the trans-conformation. Solid lines: CHARMM27 parameters with 1–4 electrostatic scaling factors: 1, brown line with crosses; 0.83, black line with filled circles; 0.6, red line with triangles; dashed blue line: c27r parameter set;<sup>14</sup> green dot-dashed line: Ryckaert-Bellemans potential with united atom GROMOS parameters.<sup>3</sup>

and compared them with the corresponding experimental data. The computed properties are: the fraction of gauche conformations in the lipid tails, the CH order parameters, and the structure factor obtained as a Fourier transform of the electron density.

The fraction of gauche conformations was computed over all 12 torsion angles of each of lipid tails. The results are shown in Table 1. As expected, the fraction of gauche-conformations is increasing upon the decrease of the scaling factor. However, already for  $\alpha_{14} = 0.8$  this fraction reaches the upper boundary of the experimental range 0.25–0.3. For  $\alpha_{14}$  between 0.6 and 0.7, which may provide a good value for the area per lipid, the fraction of gauche-conformations is becoming even greater.

The described earlier scaling of 1–4 electrostatic interactions was applied to all atoms of the lipids, so it affects the structure of both tails and the headgroups. Nevertheless, our study shows that the significant effect of this scaling appears only in the tail region. This is confirmed by the observations of average distances between different atom pairs and their distributions. For example, the average  $P$  to  $N$  distance changes from 4.51 to 4.46 Å and average  $P$  to  $C1_{\text{tail}}$  distance changes from 6.46 to 6.64 Å when the 1–4 scaling factor decreases from 1 to 0.5. At the same time, the change of the average tail length ( $C1$  to  $C14$  distance) is much stronger, from 15.1 to 12.1 Å. The tail chains acquire more gauche conformations and became shorter and thicker, thus leading to the observed increase of the area per lipid upon decrease of the scaling factor.

The order parameters of CH vectors in the lipid tails, measurable also in NMR experiments, are displayed in Figure 4. Again, the observed trend is expected: the lower scaling factor leads to a lower order parameter. The value of the scaling factor which provides the best agreement with NMR order parameters is evaluated as 0.7.

We have also computed the structure factor, which is a Fourier transform of the electron density profile in  $Z$ -direction and which is also primary data obtained in X-ray diffraction studies. The last circumstance makes the structure factor especially convenient for experimental validation of bilayer simulations.<sup>8</sup> The structure factor is computed as:<sup>15</sup>

$$F(q) = \int_{-D/2}^{D/2} (\rho(z) - \rho_w) \cos(qz) dz \quad (1)$$

where  $\rho(z)$  is the electron density profile and  $\rho_w$  is the electron density of the bulk water.

**Table 1.** Area Per Lipid and Fraction of Gauche Conformations in Lipid Tails of DMPC Bilayer Computed with Different Values of the Scaling Factor  $\alpha_{14}$  for 1–4 Electrostatic Interactions.

$\alpha_{14}$	Area per lipid	Gauche fraction
0.5	62.8	0.49
0.6	61.4	0.43
0.7	57.0	0.36
0.8	54.1	0.30
0.9	52.6	0.25
1.0	47.4	0.14
exp	60.6	0.25–0.3

Experimental data are taken from refs. 34 and 35.

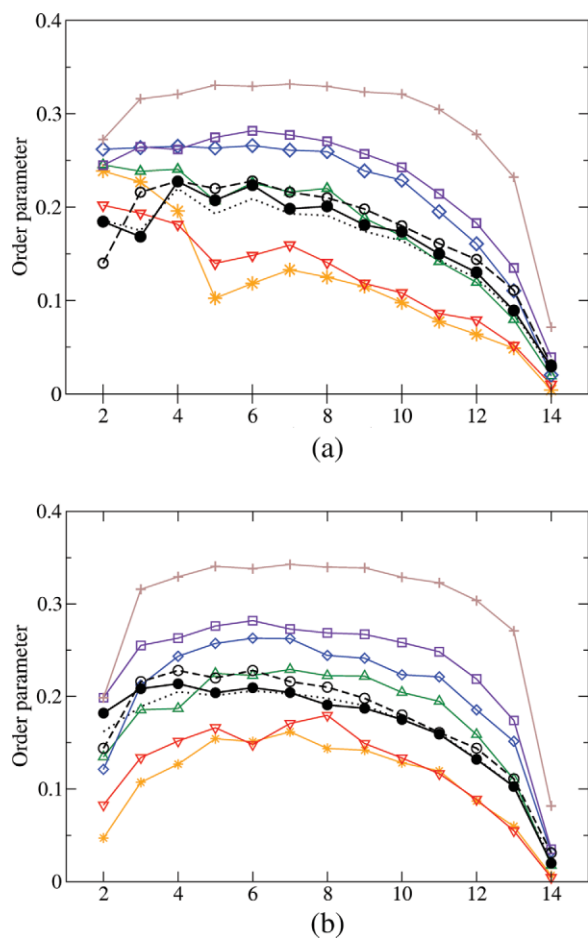


**Figure 4.** Order parameters for the lipid tails. Graphs for tail 1 are shown in (a) and for tail 2 in (b). Scaling of 1–4 parameter with 0.5, orange with stars; 0.6, red with triangles down; 0.7, green with triangles up; 0.8, blue with diamonds; 0.9, violet with squares; 1, brown with pluses. Also shown result of the New model (see Section “Simulation of DMPC Bilayer with Reparametrized Charges”) simulated with the flexible SPC water: solid black line with filled circles and with rigid TIP3P water: black dots; experimental data for liposomes from ref.<sup>36</sup> dashed black line with open circles.

The structure factors computed for each simulation are shown in Figure 5 in comparison with recent experimental data.<sup>35</sup> Also for the structure factor it can be seen that the change in scaling of the 1–4 parameter has an influence. In comparison of simulation and experimental results one should take in mind that normalization of the experimental structure factor is undetermined, that is why one should pay attention on position of maxima and zero points, as well as on relative heights of the maxima. While neither of the curves provides a perfect agreement, it can be seen that the best correspondence to experiment is given for  $\alpha_{14}$  between 0.6 and 0.7.

The differences in structure factor may be difficult to interpret, that is why we have also compared results for the electron density in real space. The results are presented in Figure 6. Similarly to the case of the structure factor, the curves most close to the experiment are those computed with the scaling factor 0.6 and 0.7. It is also clear

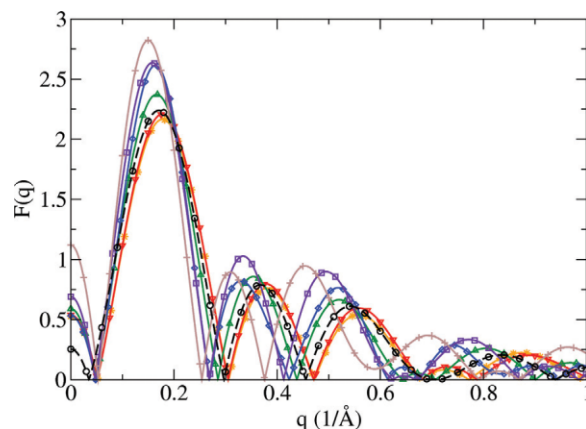


**Figure 5.** Structure factors for simulated systems with different values of 1–4 electrostatic scaling factor: 0.5, orange with stars; 0.6, red with triangles down; 0.7, green with triangles up; 0.8, blue with diamonds; 0.9, violet with squares; 1.0, brown with pluses. Experimental result<sup>15</sup> is shown as dashed black line with circles.

that larger values of the scaling factor correspond to the thicker bilayer, which is consistent with the behaviour of the average area per lipid.

### Hexadecane Simulations

It is clear from the results of the previous section that the ratio of trans/gauche conformations, determined by flexibility of the hydrocarbon chains, affects strongly properties of membrane bilayer. The reverse influence can also take place: the fact that the lipid tails are oriented preferably parallel to each other when lipids are organized in a bilayer, may enhance the fraction of trans conformations. It is, therefore, appropriately to optimize the torsion parameters for hydrocarbon chains by simulating pure hydrocarbon chains in a liquid state. We have carried out a series of simulations of liquid hexadecane at  $T = 293$  K and pressure 1 atm, described by CHARMM27

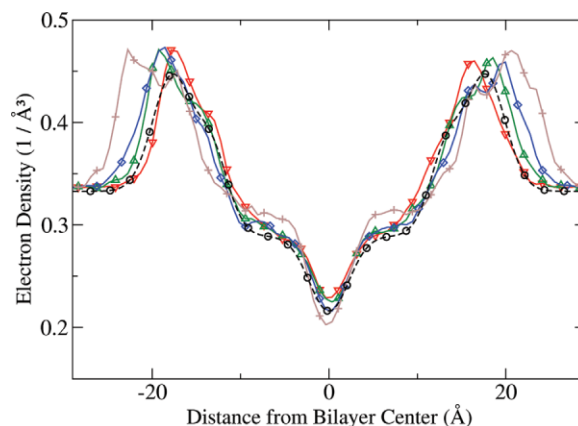


**Figure 6.** Electron density for simulated systems. 0.6, red with triangles down; 0.7, green with triangles up; 0.8, blue with diamonds; 1.0, brown with pluses; experimental result<sup>15</sup>: dashed black line with circles.

**Table 2.** Results of Hexadecane Simulations at 293 K Obtained at Different Values of Scaling Factor  $\alpha_{14}$  for 1–4 Electrostatic Interactions, with *c27r* Parameter Set and with Ryckaert-Bellemans Potential and United Atom GROMOS Parameters.

$\alpha_{14}$	$E_{\text{vap}}^a$ (kJ/mol)	Density	Fraction gauche
1 (liq)	79.0	0.777	0.26
1 (gel)	91.2	0.813	0.12
0.83	77.7	0.776	0.35
0.8	77.1	0.769	0.37
0.7	75.1	0.765	0.42
0.6	74.0	0.765	0.49
<i>c27r</i>	78.8	0.78	0.30
RB/GROMOS	78.2	0.81	0.26
stat. error	0.2	0.002	0.01
(charmm27) <sup>25</sup>	76.37	0.751	0.35
exp <sup>37</sup>	81.35 <sup>b</sup>	0.773	0.35 <sup>c</sup>

<sup>a</sup> Evaporation heat is evaluated as  $RT$  minus average intermolecular energy.

<sup>b</sup> At 25°C.

<sup>c</sup> Estimated by FTIR for tridecane.<sup>38</sup>

force field<sup>25</sup> and varying the scaling factor for 1–4 electrostatic interactions. The results for computed evaporation energy, density, and fraction of gauche conformations are presented in Table 2.

Simulations with scaling factor  $\alpha_{14} = 1$  correspond to the unmodified CHARMM27 force field. For the density and evaporation heat we obtained results similar with reported earlier,<sup>25</sup> which are also close to the experimental data. However, we obtained noticeably lower fraction of gauche conformations. Moreover, another simulation started with different initial conditions resulted in a gel (frozen) type of structure with a very low fraction of gauche defects and hydrocarbon chains oriented essentially parallel to each other. The Table 2 reports results obtained in both phases. Both “liquid” and “gel” phase simulations with  $\alpha_{14} = 1$  where further continued about 3 ns but no tendency to change the phase were registered in any of them. To completely exclude the effect of possible software deficiencies, control simulations of hexadecane were repeated by the Gromacs and NAMD simulation packages which produced the same results. Since even “liquid” phase has a too low gauche fraction, we did not pursue clarification of which phase is thermodynamically stable.

The lipid bilayer simulations carried out with scaling factor 1, which demonstrate a very low area per lipid (see Table I), show also a lipid tail structure very similar to the “gel” phase of hexadecane simulations. It is likely that falling into this phase is even more favorable in the bilayer simulations than in pure hexadecane, because of ordering influence of neighboring lipids.

We have also made comparisons with the united atom GROMOS force field with Ryckaert-Bellemans parameters for the torsion angles and the *c27r* parameter set of the CHARMM force field.<sup>14</sup> The simulation with Ryckaert-Bellemans torsion parameters provides 26% fraction of the gauche conformations which is close to the value of the unmodified *c27* parameter set of CHARMM in the liquid phase. The Ryckaert-Bellemans torsion potential was optimized empirically for butane molecules, as well as unmodified *c27* parameter set. The *c27r* parameter set is based on high-level *ab-initio* computations of several short hydrocarbons from pentane to

heptane. This lead to some decrease and broadening of the potential well for gauche conformations, and, according to our simulations, to increase of the gauche fraction in liquid hexadecane to about 30%.

The known experimental value of the fraction of gauche conformations in aliphatic hydrocarbon chains is estimated as 35%. A reservation should be made that this value, deduced from FTIR measurements for tridecane,<sup>38</sup> may be subject of some uncertainty due to difficulties in interpretation of experimental data. However, it is well correlated with estimations of 25–30% of gauche defects in aliphatic tails of lipids,<sup>33,34</sup> where the fraction of trans-conformations may be enhanced due to ordering effect of the liquid crystalline phase. In absence of accurate experimental data, an alternative may be to refer to high-level *ab-initio* calculations. The *ab-initio* calculations, made in work<sup>14</sup> for pentane, hexane, and heptane, resulted in formulation of the revised *c27r* force field with somewhat lower energy of gauche conformation comparing to the unmodified *c27* torsion potential, which was earlier parametrized in *ab-initio* computations for butane.<sup>25</sup> Correspondingly, the *c27r* parameter set yields 30% gauche fraction for hexadecane comparing to 26% obtained in the liquid phase with the unmodified *c27* force field, see Table 2. Further analysis of Table 3 of work<sup>14</sup> reveals, that there is still a trend of decreasing the difference between the gauche and trans *ab-initio* energies while going from pentane to heptane. It is therefore not unrealistic to suggest that for longer hydrocarbon chains, the energy difference between trans and gauche conformations will be lower than that in the *c27r* parameter set, leading to higher than 30% fraction of the gauche conformations.

As we discussed earlier, the trans/gauche ratio can be very conveniently varied by a change of the 1–4 scaling factor. The results in

**Table 3.** Partial Atom Charges for DMPC Lipid.

Atom	CHARMM type	A	B	C	$\delta q$
N	NTL	−0.6	0.21	0.25	0.04
$C_\gamma$	CTL5	−0.35	−0.43	−0.44	0.03
$H_\gamma$	HTL5	0.25	0.21	0.20	0.01
$C_\beta$	CTL2	−0.1	−0.35	−0.25	0.14
$H_\beta$	HTL2	0.25	0.21	0.14	0.05
$C_\alpha$	CTL2	−0.08	0.20	0.22	0.17
$H_\alpha$	HTL2	0.09	0.03	0.06	0.05
$O_\alpha, O_{g3}$	OSL	−0.57	−0.42	−0.54	0.04
P	PL	1.50	0.83	1.59	0.09
$O_P$	O2L	−0.78	−0.71	−0.91	0.03
$C_{g3}$	CTL2	−0.08	0.11	−0.16	0.16
$H_{g3}$	HTL2	0.09	0.03	0.12	0.04
$C_{g2}$	CTL1	0.04	0.08	0.51	0.16
$H_{g2}$	HTL1	0.09	0.08	0.03	0.04
$C_{g1}$	CTL2	−0.05	0.03	0.11	0.10
$H_{g1}$	HTL2	0.09	0.08	0.06	0.03
$O_{g1}, O_{g2}$	OSL	−0.34	−0.39	−0.54	0.04
$C_1$	CL	0.63	0.88	0.82	0.03
$O_e$	OBL	−0.52	−0.55	−0.61	0.02
$C_2$	CTL2	−0.08	−0.58	−0.09	0.05
$H_2$	HTL2	0.09	0.19	0.05	0.02

A, original CHARMM charges; B, MP2-level calculation for small fragments; C, computed at the Hartree-Fock level as an average over 10 randomly chosen configurations for the whole headgroup, with the corresponding variance given in column  $\delta q$ . See Figure 1 for the atom notations.

Table 2 shows similar increase of the gauche fraction upon decrease of the scaling factor, as those observed in the bilayer simulations. Clearly, the scaling factor 0.6, which provided the best area per lipid in Table 1, results in an unacceptably high gauche fraction. The value of the scaling factor which provides the best coincidence with the experiment seems to be 0.83. It may be worth to note that just this value of the scaling factor for 1–4 electrostatic interaction is adopted as a default in the AMBER force field.

Data in Table 2 show that the density and evaporation heat of hexadecane depend very little on the 1–4 scaling factor, remaining in acceptable agreement with experiment. We therefore adopted 0.83 as the optimal value of the scaling factor for 1–4 electrostatic interactions, under condition that original CHARMM27 force field is used for description of other hydrocarbon parameters.

### Optimization of Atom Charges

Simulations of DMPC bilayer described in Section “Effect of Scaling of 1–4 Electrostatic Interactions on Bilayer Structure” show that choice of the electrostatic scaling factor 0.83 does not allow to bring the area per lipid and other bilayer properties in agreement with experiment. We therefore performed the next step in optimization of the force field parameters, namely we recalculated all partial atomic charges of the lipid headgroup. In development of the original CHARMM force field, the partial charges were computed in *ab-initio* calculations (on typically HF/6-31(d) level) of small molecular fragments in presence of one water molecule, with subsequent scaling of these charges to fit experimental data for these model components.<sup>39</sup> It may be argued however that after building a bigger molecule from small fragments, some redistribution of charges between the fragments may occur. We therefore recalculated partial atomic charges in two ways. First, we split the lipid headgroup on small fragments (choline group, phosphate group with  $\alpha$  and  $g_3$  methyl groups, and two ester moieties with  $g_1$  or  $g_2$  carbons), substituting hydrogens instead of broken bonds, and recalculated atom charges using the MP2-level *ab-initio* theory with 6-311+(2d,p) basis set. The computations were made using GAMESS package.<sup>40</sup> In these calculations, the choline group had the total charge +1e, the charge –1e was prescribed to the phosphate group while the glycerol-ester group was neutral. Symmetrization of charges of similar atoms was made afterwards. The computations were carried out for the optimized geometries of these fragments and the electrostatic potential fitting was used to derive the partial atomic charges. This set of charges is presented in column “B” of Table 3.

In another approach, calculations were carried out for the whole lipid headgroup including ester moieties. Since the partial charges depend on the molecular conformation which for lipid headgroups changes significantly, the computations were carried out for a number of different lipid configurations randomly chosen from the molecular dynamics trajectory. In our work, we chose ten configurations of lipids from the described above simulation with the electrostatic scaling factor 0.8. The tails were removed after the second carbon atom in each tail, and substituted by hydrogen atoms. *Ab-initio* computations of this series were carried out on the HF/6-311(d,p) level using Gaussian-03 package.<sup>41</sup> For each configuration, charges were computed using electrostatic potential

fitting and averaged over symmetrical or similar atoms. Average values of the computed charges and variances taken over the 10 chosen configurations are shown in columns “C” and “ $\delta q$ ” of Table 3, respectively.

Table 3 shows that the charge on some atoms ( $\alpha$ ,  $\beta$ , and glycerol carbons) varies strongly depending on molecular conformation. Often a special restrain procedure (for example, RESP algorithm<sup>42</sup>) is introduced to avoid such an influence, which may be important if only a single (typically, optimized geometry) conformation is used for the calculations. We used, instead of RESP procedure, averaging over ensemble of typical conformations taken from the molecular dynamics trajectory. One can also note from the analysis of individual conformations, that charges of different groups of neighboring atoms are much less conformation dependent than that for individual atoms. The total charge of the choline group (including  $\beta$  methyl group) is 0.76 with 0.04 variance. For the phosphate moiety, including  $\alpha$  and  $g_3$  methyl groups, the charge is  $-0.89 \pm 0.05$  while for the ester group (including  $g_1$  and  $g_2$  of glycerol and the second  $\text{CH}_2$  groups of each tail) the charge is  $+0.13 \pm 0.04$ . For comparison, the total charge of these moieties in the original CHARMM27 force field is +1, –1, and 0, respectively. It is interesting that in work of Sonne et al.,<sup>13</sup> where similar approach was used for DPPC lipid headgroup and computations were carried out at the RHF/6-31G(d) level, distribution of charges over the three groups turned out to be very similar to our: 0.74 for choline, –0.87 for phosphate, and +0.13 for the glycerol-ester part. It is clear, that after putting the corresponding atom groups in a lipid molecule together, some redistribution of charge occurs, with the most noticeable move of a part of positive charge from the choline to the ester group of the lipid. Given the fact that behavior of bilayer is very sensitive to electrostatic (dipole) interactions,<sup>5</sup> such redistribution of charges may affect the bilayer properties which is demonstrated in the next section.

### Simulation of DMPC Bilayer with Reparametrized Charges

Two simulations of DMPC bilayer with “B” and “C” sets of charges given in Table 3, with 0.83 scaling factor for 1–4 electrostatic interactions, and in presence of flexible SPC water were carried out, starting from a configuration generated in the simulation with the original CHARMM charges and 0.8 scaling factor. For simulation with set of charges “B”, the area per lipid is way too small compared to experiment. It exhibits behavior similar to that obtained with non-modified CHARMM charges and 0.8 or 0.9 scaling factor for 1–4 electrostatic interactions, see Figure 7. Because of this we do not present the results from this simulation further but instead focus on simulation with the set of charges “C” which we also call “New model”, or “c27m” parameter set.

The “New model” was simulated during 75 ns and evolution of its area per lipid is shown in Figure 7. Also shown are running averages over 10 ns windows. After about 30 ns of simulation the area seems to reach a stable level of  $59.9 \pm 0.5 \text{ \AA}^2$ , which is practically coincides with the most recent experimental value  $60.6 \text{ \AA}^2$ .<sup>35</sup>

Given the fact that the CHARMM force field was parametrized for the rigid TIP3P water model and that the TIP3P water is used in a wider range of molecular dynamics packages, we carried out

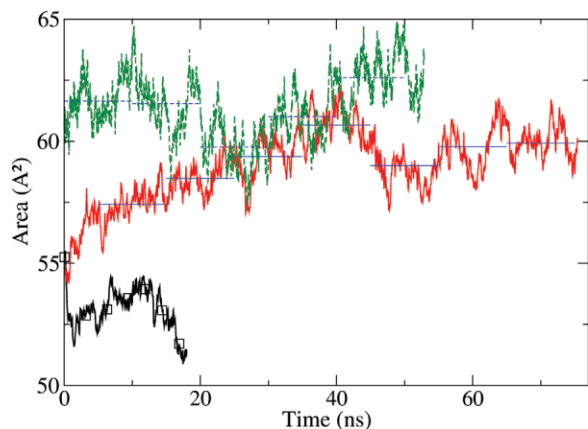


**Figure 7.** Area per lipid for systems with partial atom charges “B” (black line with squares) and “C” (new model), simulated with flexible SPC water (solid red line), and with rigid TIP3P water (dashed green line). For model “C,” averages over 10 ns windows are shown as blue horizontal lines. [Color figure can be viewed in the online issue, which is available at [www.interscience.wiley.com](http://www.interscience.wiley.com).]

an additional 50 ns simulation of the new DMPC lipid model with TIP3P water model, taking the last configuration of the simulation with flexible SPC water as a starting configuration of the simulation with TIP3P water. The last mentioned simulation has been carried out using NAMD simulation package, with time step 2 fs, rigid water geometry and rigid CH bonds in lipids. Other simulation parameters were essentially the same as in simulations with flexible SPC water. Evolution of the area per lipid for this simulation is also displayed in Figure 7. Averaging over the last 40 ns yields an average area  $61.3 \pm 0.7 \text{ \AA}^2$ , which, being slightly above the result of the flexible SPC water, is again in a very good agreement with the experimental value.

We have calculated a number of properties of the simulated bilayer taking average over the last 40 ns of these simulations.

As can be seen in Figure 4, the tail order parameters for both tail 1 and tail 2 are also in a very good agreement with experiment, though simulation with TIP3P water shows slightly lower

order parameters. The results are close to the case of scaling factor  $\alpha_{14} = 0.7$  with unmodified charges, but the overall shape of the order parameter curve for the New model is much closer to the experimental one. In Table 4 we also present order parameters for the lipid head group. It can be seen that all order parameters correspond well to the experiment. A possible exception is the order parameters for the *g3R* carbon which, according to paper,<sup>36</sup> is positive while we obtained negative order parameters for both *g3* CH bonds. However, another work<sup>43</sup> reports no splitting between *g3* order parameters and provides a negative value close to our results for both *g3R* and *g3S*.

The structure factor for the New model is presented in Figure 8. The original values of the experimental structure factor<sup>15</sup> were scaled in order to fit better to the first maxima of the simulated structure factors. Agreement between the experimental and simulated results is generally good for the two simulations, with somewhat larger deviations for the large values of the wave number. Important is that the positions of maxima and zero points are well correspond to the experimental curve.

To shed more light onto the possible differences in the bilayer structure, we plotted in Figure 9 the electron density profiles for the performed simulations. For the newly developed lipid model, simulated in presence of the both water models, the electron density is very similar to the experimental one. The new model reproduces well the positions of maxima of the electron density in the lipid headgroup region as well as the overall shape of the density in the membrane interior. Noticeable differences between simulations with the two water models are seen only near the maxima of the electron density, which corresponds to the headgroup region with many contacts between lipids and water. The flexible SPC water shows somewhat higher association with the polar atoms of the headgroups, which is related to the possibility for intramolecular bonds to stretch and to make the hydrogen bond structure stronger. This leads to somewhat stronger maxima of the electron density and somewhat lower area per lipid, in comparison with simulations employing TIP3P water. One can also make an observation, that in the case of SPC water the simulated electron density follows the experimental curve more closely (note a better shape of the plateau at 5–9 Å from the membrane center, a weakly expressed shoulder at about 14 Å, a bit lower

**Table 4.** Order Parameters for the Lipid Headgroup and Glycerol Moiety.

	Original CHARMM charges					New model		Experiment	
	0.5	0.6	0.7	0.8	0.9	SPCf	TIP3P	Ref. 36	Ref. 43
<i>g1R</i>	−0.227	−0.156	−0.195	−0.211	−0.197	−0.132	−0.079	−0.103/0.152*	−0.15
<i>g1S</i>	0.025	0.026	0.008	0.02	0.101	0.013	0.016	0.005/−	0
<i>g2</i>	−0.253	−0.222	−0.256	−0.268	−0.278	−0.182	−0.163	−0.143/0.212*	−0.20
<i>g3R</i>	−0.228	−0.241	−0.274	−0.268	−0.289	−0.291	−0.285	0.156/0.212*	−0.23
<i>g3S</i>	−0.295	−0.246	−0.273	−0.293	−0.299	−0.206	−0.181	−0.167/0.224*	−0.23
$\alpha$	0.114	0.107	0.112	0.102	0.091	0.088	0.097	0.035/0.050	0.04
$\beta$	−0.023	0.005	−0.011	−0.035	−0.03	−0.046	−0.030	−0.025/−0.042	−0.03

The first five columns show order parameters computed with the original CHARMM charges and different values of the 1–4 electrostatic scaling factor; the next two columns show result for the New model (see Section “Simulation of DMPC Bilayer with Reparametrized Charges”) in presence of two different water models, and the last two columns give experimental order parameters from ref. 36 (measured for bicelles/liposomes) and from ref. 43. An asterisk indicates that only the absolute value was measured. Statistical error for all values is within 0.005.

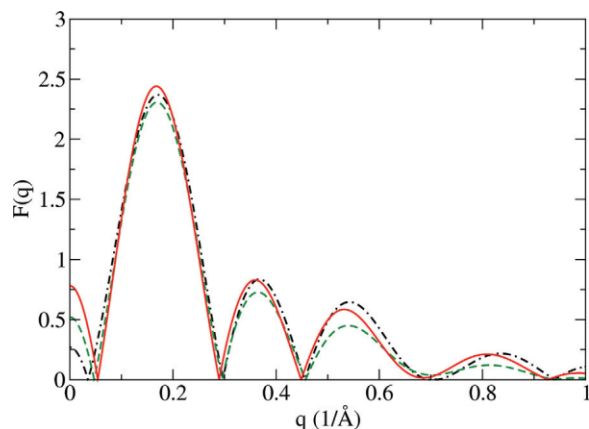


**Figure 8.** Structure factors for the new model simulated with flexible SPC water (red solid line) and with rigid TIP3P water (green dashed line). The experimental structure factor<sup>15</sup> is shown as black dot-dashed line. [Color figure can be viewed in the online issue, which is available at [www.interscience.wiley.com](http://www.interscience.wiley.com).]

minimum of the density in the middle of membrane). The differences are, however, mostly within the statistical error which can be evaluated from the asymmetry of the right and left parts of the plot.

For comparison, we also displayed the electron density from our previous simulation of DMPC bilayer with GROMOS force field<sup>9</sup> carried out at the same conditions (temperature 303 K, full hydration, and zero tension). GROMOS electron density deviate more from the experimental curve than our modified CHARMM force field. One can see clear improvements in reproduction of the experimental density profile in the case of the modified CHARMM force field developed in the present work.

Previous detailed studies of the electron density profile and structure factor in lipid bilayers<sup>8,15</sup> also demonstrated rather good, similar to the observed in our work, agreement of these properties to the experiment in cases when the simulated lipid area was correct. However, simulations of DMPC or DPPC lipids at constant pressure and unmodified CHARMM27 force field do not provide the correct lipid area. Note also, that other properties, such as order parameters and gauche-fraction, need to be taken into account while evaluating the force field. For example, our simulation with unmodified charges and 0.6 electrostatic scaling factor (see Section “Effect of Scaling of 1–4 Electrostatic Interactions on Bilayer Structure”) provides good results for the average lipid area, structure factor, and the electron density, but shows considerable disagreement with experiment for the order parameters and the gauche-fraction.

## Discussion

We have modified CHARMM force field for simulations of DMPC lipid bilayers which provides substantial improvement in reproduction of available experimental data.

The most important parameter, area per lipid at zero tension, is well reproduced by the new model. Also, a good agreement has been observed for the order parameters, fraction of gauche defects, structure factor, and the electron density. It is worth to note, that

the experimental area per lipid was not used in parametrization of the model. Instead, the parametrization consisted in improvement of description of the two main parts of the lipids: hydrocarbon tails and the headgroup. Changing of the 1–4 scaling factor for electrostatic interactions provides correct description of alkanes chains in the membrane interior, which is also confirmed by the liquid hexadecane simulations. Recalculation of charges within the whole lipid head group results in a more realistic overall charge distribution within a separate lipid molecule, as well as within the bilayer as a whole. Both factors increase the average area per lipid, bringing it close to the experimental value.

In the new set of charges, overall charges of the choline and phosphate groups are somewhat below 1, which reduces the in-plane dipole moments of the headgroup. Simultaneously, because of the shift of a positive charge to the glycerol-ester moiety, a dipole normal to the bilayer appears. Since interactions of in-plane dipoles are mostly attractive while that of normal dipoles are mostly repulsive, the both factors lead to increase of repulsion between the headgroups and to increase of the area per lipid. This argumentation is confirmed by comparison of results of simulations carried out with unmodified CHARMM charges, with set of charges “B” (without charge redistribution between the groups), and with the set of charges “C” (the New model). Also, similar to our model redistribution of charges has been obtained in recent work of Sonne et al.<sup>13</sup> which has also led to increase of the area per lipid for DPPC bilayer in comparison with the original CHARMM force field. However, in the work<sup>13</sup> the 1–4 electrostatic scaling factor was not used, and the area per lipid for DPPC obtained in that work was still below the experimental one, likely because the lipid tails remained too rigid.

Similarly, if one increases tails flexibility while keeping the original CHARMM charges, as it was done in the c27r parameter set,<sup>14</sup> the area per lipid simulated at zero tension still remains too low.<sup>15,17</sup> Our simulation described in Section “Effect of Scaling of 1–4 Electrostatic Interactions on Bilayer Structure” shows,

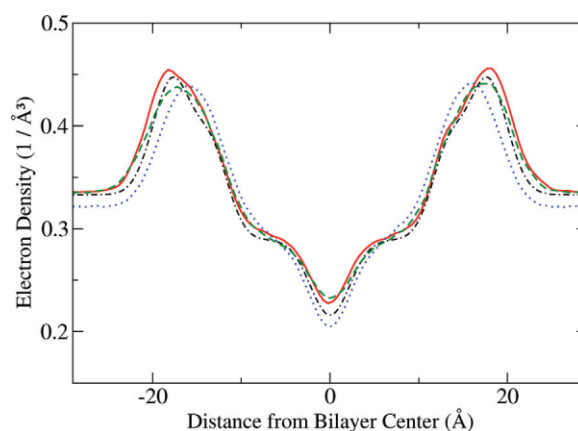


**Figure 9.** Electron density for the new model simulated with flexible SPC water (red solid line) and with rigid TIP3P water (green dashed line). The experimental structure factor<sup>15</sup> is shown as thin black dot-dashed line and result of simulation with the GROMOS force field from work<sup>9</sup> as blue dots. [Color figure can be viewed in the online issue, which is available at [www.interscience.wiley.com](http://www.interscience.wiley.com).]

that in order to reach the experimental value of the area per lipid (at the condition of original charges), tails flexibility should be increased to an unrealistic level. Only combination of the two suggested modifications can provide consistent behavior of the lipid bilayer.

While modification of charges in the lipid headgroup was made on the basis of *ab-initio* calculations, the scaling factor for 1–4 electrostatic interactions was derived in a purely empirical manner by fitting the gauche fraction for liquid hexadecane. Accurate *ab-initio* computations of the torsion potential of long hydrocarbon chains along the lines described by Klauda et al.<sup>14</sup> may be preferable, while used in our work scaling of 1–4 interactions may be considered as a cheap but working solution. It is also interesting to note, that obtained in our work optimal value of the 1–4 electrostatic scaling factor (given as 1/1.2) was recommended in the AMBER forces field.<sup>44,45</sup> This recommendation was made on the basis of studies of many different organic compounds with a purpose to provide a possibly better transferability of the force field parameters when the charges are computed in *ab-initio* calculations. This may give some justification of keeping the same scaling factor for 1–4 electrostatic interactions in the headgroup, where all the charges were determined from *ab-initio* computations.

Simulations of the new DMPC model have been done in presence of both flexible SPC and rigid TIP3P water, which turned out to provide results very close to each other. Simulation with TIP3P water yields a slightly higher area per lipid and a bit more disordered structures, but the difference in results obtained with these two models are just about the statistical error. This indicate a certain freedom in a choice of water model and possibility to accommodate the model which is the most suitable for a given study. While rigid water is conventionally used in many simulation packages, the flexible SPC model have a number of certain advantages, such as correct dielectric constant and possibility to change geometry upon a change in the environment, mimicking in this way polarizability. Note also that implementation of fully flexible molecular models does not bring significant increase of the simulation time if a multiple time step algorithm is used in the simulations.

Finally we would like to conclude that the model developed in our work provides not only perfect agreement for the area per lipid. For the structure factor and electron density we also get results in good agreement with the experiment. Clear improvement is also seen for the order parameters, including those in the headgroup part of the lipid. The model can be recommended for simulations of lipids of similar structure such as DLPC or DPPC. Also, the suggested approach can be used for improvements in parametrization of other types of lipids.

## Acknowledgements

Computer time has been granted by the Center for Parallel Computing at the Royal Institute of Technology, Stockholm, and the High Performance Computing Center North, Umeå. We are thankful to Prof. J. Nagle for providing us numerical data for the structure factors and electron density and for valuable comments about the manuscript.

## References

1. Marrink, S. J.; Berendsen, H. J. C. *J Phys Chem* 1994, 98, 4155.
2. Tieleman, D. P.; Berendsen, H. J. C. *J Chem Phys* 1996, 105, 4871.
3. Berger, O.; Edholm, O.; Jähnig, F. *Biophys J* 1997, 72, 2002.
4. Lindahl, E.; Edholm, O. *Biophys J* 2000, 79, 426.
5. Wohrlert, J.; Edholm, O. *Biophys J* 2004, 87, 2433.
6. Falck, E.; Patra, M.; Karttunen, M.; Hyvönen, M. T.; Vattulainen, I. *Biophys J* 2004, 87, 1076.
7. de Vries, A. H.; Chandrasekhar, I.; van Gunsteren, W. F.; Hünenberger, P. H. *J Phys Chem B* 2005, 109, 11643.
8. Benz, R. W.; Castro-Roman, F.; Tobias, D. J.; White, S. H. *Biophys J* 2005, 88, 805.
9. Högberg, C.-J.; Lyubartsev, A. P. *J Phys Chem B* 2006, 110, 14326.
10. Pohle, W.; Gauger, D. R.; Bohl, R.; Mrazkova, E.; Hobza, P. *Biopolymers* 2004, 74, 27.
11. Mackerell, A. D.; Wiorcikiewicz-Kuczera, J.; Karplus, M. *J Am Chem Soc* 1995, 117, 11946.
12. Hyvönen, M. T.; Kovanen, P. T. *Eur Biophys J* 2005, 34, 294.
13. Sonne, J.; Jensen, M. Ø.; Hansen, F. Y.; Hemmingsen, L.; Peters, G. H. *Biophys J* 2007, 92, 4157.
14. Klauda, J. B.; Brooks, B. R.; MacKerell, A. D.; Venable, R. M.; Pastor, R. W. *J Phys Chem B* 2005, 109, 5300.
15. Klauda, J. B.; Kučerka, N.; Brooks, B. R.; Pastor, R. W.; Nagle, J. F. *Biophys J* 2006, 90, 2796.
16. Sonne, J.; Hansen, F. Y.; Peters, G. H. *J Chem Phys* 2005, 122, 124903.
17. Pedersen, U. R.; Peters, G. H.; Westh, P. *Biophys Chem* 2007, 125, 104.
18. Jorgensen, W. L.; Chandrasekhar, J.; Madura, J. D.; Impey, R. W.; Klein, M. L. *J Chem Phys* 1983, 79, 926.
19. Höchtel, P.; Boresch, S.; Bitomsky, W.; Steinhauser, O. *J Chem Phys* 1998, 109, 4927.
20. Anezo, C.; de Vries, A. H.; Höltje, H.-D.; Tieleman, D. P.; Marrink, S.-J. *J Phys Chem B* 2003, 107, 9424.
21. Price, D. J.; Brooks, C. L. *J Chem Phys* 2004, 121, 10096.
22. Toukan, K.; Rahman, A. *Phys Rev B* 1985, 31, 2643.
23. Anderson, J.; Ullio, J. J.; Yip, S. *J Chem Phys* 1987, 87, 1726.
24. Nikitin, A. M.; Lyubartsev, A. P. *J Comput Chem* 2007, 28, 2020.
25. Feller, S. E.; MacKerell, A. D. *J Phys Chem B* 2000, 104, 7510.
26. Allen, M. P.; Tildesley, D. J. *Computer Simulations of Liquid*, 2nd ed.; Clarendon: Oxford, 1987.
27. Martyna, G. J.; Tuckerman, M. E.; Tobias, D. J.; Klein, M. L. *Mol Phys* 1996, 87, 1117.
28. Tuckerman, M.; Berne, B. J.; Martyna, G. J. *J Chem Phys* 1992, 97, 1990.
29. Ewald, P. *Ann Phys* 1921, 64, 253.
30. Lyubartsev, A. P.; Laaksonen, A. *Comput Phys Commun* 2000, 128, 565.
31. Lindahl, E.; Hess, B.; van der Spoel, D. *J Mol Model* 2001, 7, 306.
32. Kale, L.; Skeel, R.; Bhandarkar, M.; Brunner, R.; Gursoy, A.; Krawetz, N.; Phillips, J.; Shinozaki, A.; Varadarajan, K.; Schulten, K. *J Comp Phys* 1999, 151, 283.
33. Mendelsohn, R.; Davies, M. A.; Brauner, J. W.; Schuster, H. F.; Diuhy, R. A. *Biochemistry* 1989, 28, 8934.
34. Casal, H. L.; McElhaney, R. N. *Biochemistry* 1990, 29, 5423.
35. Kučerka, N.; Liu, Y.; Chu, N.; Petrache, H. I.; Tristram-Nagle, S.; Nagle, J. F. *Biophys J* 2005, 88, 2626.
36. Aussenac, F.; Laguerre, M.; Schmitter, J.; Dufourc, E. *Langmuir* 2003, 19, 10468.
37. Lide, D. R., Ed. *CRC Handbook of Chemistry and Physics*, 81st ed., CRC Press: New York, 2000.
38. Holler, F.; Callis, J. B. *J Phys Chem* 1989, 89, 2053.
39. MacKerell, A. D.; Bashford, D.; Bellott, M.; Dunbrack, R. L.; Evanseck, J. D.; Field, M. J.; Fisher, S.; Gao, J.; Ha, S.; Joseph-McCarthy, D.; Kuchnir, L.; Kuczera, K.; Lau, F. T. K.; Mattos, C.; Michnick, S.; Ngo, T.;

- Nguyen, D. T.; Prodhom, B.; Reiher, W. E. III; Roux, B.; Schlenkrich, M.; Smith, J. C.; Stote, R.; Straub, J.; Watanabe, M.; Wiorkiewicz-Kuczera, J.; Yin, D.; Karplus, M. *J Phys Chem B* 1998, 102, 3586.
40. Schmidt, M. W.; Baldrige, K. K.; Boatz, J. A.; Elbert, S. T.; Gordon, M. S.; Jensen, J. H.; Koseki, S.; Matsunaga, N.; Nguyen, K. A.; Su, S. J.; Windus, T. L.; Dupuis, M.; Montgomery, J. A. *J Comput Chem* 1993, 14, 1347.
41. Frisch, M. J.; Trucks, G. W.; Schlegel, H. B.; Scuseria, G.; Robb, M. A.; Cheeseman, J. R.; J. A. Montgomery, J.; Vreven, T.; Kudin, K. N.; Burant, J. C.; Millam, J. M.; Iyengar, S. S.; Tomasi, J.; Barone, V.; Mennucci, B.; Cossi, M.; Scalmani, G.; Rega, N.; Petersson, G. A.; Nakatsuji, H.; Hada, M.; Ehara, M.; Toyota, K.; Fukuda, R.; Hasegawa, J.; Ishida, M.; Nakajima, T.; Honda, Y.; Kitao, O.; Nakai, H.; Klene, M.; Li, X.; Knox, J. E.; Hratchian, H. P.; Cross, J. B.; Adamo, C.; Jaramillo, J.; Gomperts, R.; Stratmann, R. E.; Yazyev, O.; Austin, A. J.; Cammi, R.; Pomelli, C.; Ochterski, J. W.; Ayala, P. Y.; Morokuma, K.; Voth, G. A.; Salvador, P.; Dannenberg, J. J.; Zakrzewski, V. G.; Dapprich, S.; Daniels, A. D.; Strain, M. C.; Farkas, O.; Malick, D. K.; Rabuck, A. D.; Raghavachari, K.; Foresman, J. B.; Ortiz, J. V.; Cui, Q.; Baboul, A. G.; Clifford, S.; Cioslowski, J.; Stefanov, B. B.; Liu, G.; Liashenko, A.; Piskorz, P.; Komaromi, I.; Martin, R. L.; Fox, D. J.; Keith, T.; Al-Laham, M. A.; Peng, C. Y.; Nanayakkara, A.; Challacombe, M.; Gill, P. M. W.; Johnson, B.; Chen, W.; Wong, M. W.; Gonzales, C.; Pople, J. A. *Gaussian 03*; Gaussian Inc., 2003.
42. Bayly, C. I.; Cieplak, P.; Cornell, W.; Kollman, P. *J Phys Chem* 1993, 97, 10269.
43. Gross, J. D.; Warschawski, D. E.; Griffin, R. G. *J Am Chem Soc* 1997, 119, 796.
44. Cornell, W. D.; Cieplak, P.; Bayly, C. I.; Kollman, P. A. *J Am Chem Soc* 1993, 115, 9620.
45. Cornell, W. D.; Cieplak, P.; Bayly, C. I.; Gould, I. R.; Merz, K. M.; Ferguson, D. M.; Spellmeyer, D. C.; Fox, T.; Caldwell, J. W.; Kollman, P. A. *J Am Chem Soc* 1995, 117, 5179.